Received: 26 October 2022 | Revised: 18 March 2023 | Accepted: 31 March 2023

DOI: 10.1002/hyp.14870

RESEARCH ARTICLE

WILEY

Accuracy verification of optical fingerprinting methods in sediment tracing study

Dan Chen[1] | Wei Dai[1] | Mengjie Li[1] | Bing Wang[1] | Yi Zeng[1,2] | Lingshan Ni[1,2] | Nufang Fang[1,2] | Zhihua Shi[2,3]

[1]State Key Laboratory of Soil Erosion and Dryland Farming on the Loess Plateau, Institute of Soil and Water Conservation, Northwest A&F University, Yangling, Shaanxi Province, The People's Republic of China

[2]Institute of Soil and Water Conservation, Chinese Academy of Sciences and Ministry of Water Resources, Yangling, Shaanxi Province, The People's Republic of China

[3]College of Resources and Environment, Huazhong Agricultural University, Wuhan, The People's Republic of China

Correspondence
Lingshan Ni, Institute of Soil and Water Conservation, Northwest A&F University, 26 Xinong Road, Yangling, Shaanxi Province 712100, The People's Republic of China.
Email: lsni@ms.iswc.ac.cn

Funding information
Fundamental Research Funds for the Central Universities, Grant/Award Numbers: 2022HXZX002, 2452020206; National Natural Science Foundation of China, Grant/Award Numbers: 42107361, 42177335, 41930755

Abstract

Sediment fingerprints have been widely used in source identification studies. Optical features have become a powerful substitute for traditional fingerprints in recent years due to their fast measurement and low analysis costs. However, the accuracy of optical fingerprinting methods has received little attention. Here, artificial mixing and indoor scouring experiments were carried out to compare and assess the accuracy of optical fingerprinting results using three spectroscopic ranges [visible (VIS), near-infrared (NIR), and mid-infrared (MIR) spectroscopy] in multivariate models and using 19 colour parameters [such as red (R), green (G) and blue (B) in an RGB system; virtual component X (X), brightness (Y) and virtual component Z (Z) in a CIE XYZ system and so on] coupled with the conventional method. Furthermore, we examined how sediment sorting (particle sorting and organic matter enrichment) affects the accuracy of source apportionments. The results showed that VIS, NIR and MIR spectroscopic tracers presented high accuracy in scouring and artificial mixtures, with mean absolute error (MAE) values of 4.98% and 5.91%. In contrast, the colour parameters had weak performances in two experiments (MAE = 16.83% and 15.05%). Additionally, similar fingerprinting results of the scouring mixtures (MAE = 7.95%) and artificial mixtures (MAE = 8.20%) indicated that slight particle sorting and organic matter enrichment have little effect on the accuracy of optical fingerprinting results. Our study shows that sediment fingerprinting based on optical features, especially three spectroscopic ranges, has good applicability in sediment source identification.

KEYWORDS
artificial mixtures, colour parameters, indoor simulated scouring experiments, sediment fingerprinting, spectroscopic features

1 | INTRODUCTION

Accelerated soil erosion processes have result in on-site environmental problems such as the decline of land productivity by removing the topsoil rich in organic matter (Amundson et al., 2015; Syvitski et al., 2022), and off-site problems due to the entry of sediment into rivers and reservoirs leading to siltation and a decline in water quality (Collins et al., 2020). Determining the source of sediments is an important prerequisite for the control of soil erosion and its associated environmental problems (Poesen, 2018). When the sediment source is accurately quantified, targeted watershed management can be carried out, which is an essential tool for policymakers involved in soil conservation decision-making (Evrard et al., 2022; Xu et al., 2022).

Sediment fingerprinting is a widely used method for determining the relative contribution of potential sediment sources (Collins et al., 2020; Pulley & Collins, 2022). The basis of this method is to

select soil properties that make it possible to distinguish sediment sources as potential fingerprints, then combine them with unmixing models to quantify the contribution of potential sediment sources. To date, many soil properties have been used as fingerprints, such as soil physical properties, radionuclides, geochemical elements, and biomarkers (Chen et al., 2019; Evrard et al., 2019; Ni et al., 2017; Shi et al., 2019). However, the measurement of traditional tracers was not only destructive to soil samples, but also time-consuming and expensive (Tiecher et al., 2015, 2021). This resulted in limited large-scale application of traditional tracers in the field environment.

Optical features can be used as a powerful alternative to traditional fingerprints due to their vast quantities of information, potential for rapid and low-cost analysis, and their non-destructive nature (Tiecher et al., 2021). Poulenard et al. (2009, 2012) were the first to successfully use mid-infrared spectra for tracing surface and channel sources as well as various lithological sources. Since then, many different spectral bands, including visible (Lake et al., 2022; Martínez-Carreras et al., 2010), near-infrared (Collins et al., 2013, 2014; Tiecher et al., 2016), mid-infrared spectroscopy (Ni et al., 2019; Vercruysse & Grabowski, 2018), and combinations of these spectroscopies (Farias Amorim et al., 2021; Verheyen et al., 2014) have been used to trace sediment sources.

Although optical fingerprinting methods have been successfully applied recently in the field, the accuracy of these tracers has not been well evaluated (Collins et al., 2017; Laceby et al., 2017). In field environments, it is difficult to verify the reliability of estimated results of sediment sources because of the limitations of measurement means and cost (Collins & Walling, 2004). A pre-known proportion of artificial mixtures has become a good solution for verifying the accuracy of sediment fingerprinting results (Gaspar et al., 2019; Laceby et al., 2015; Sherriff et al., 2015). Haddadchi et al. (2014) used artificial mixtures to evaluate the accuracy of different mixing model outputs. Laceby et al. (2015) illustrated the impact of tracer selection by using different methods in tracing studies. Additionally, different proportions of artificial mixtures have been used to calibrate and validate spectroscopic models (Poulenard et al., 2009, 2012). However, accuracy verification studies using only artificial mixing experiments have been incomplete, as mixing experiments do not represent the possible changes to sediment particle size distribution and organic matter content which can occur during erosion transport and deposition of sediment in the field environment (Zhang et al., 2021). Therefore, indoor scouring experiments should also be considered to simulate the real transport process and dry and wet changes of sediments on slopes under controllable conditions.

In this study, detailed artificial mixtures and indoor simulated scouring experiments were carried out, aiming to (1) compare and assess the accuracy of fingerprinting results using colour parameters coupled with conventional fingerprinting methods using multivariate methods based on three spectroscopic ranges (VIS, NIR, and MIR spectroscopy), and (2) analyse the effect of particle sorting and organic matter enrichment on the accuracy of optical fingerprinting during slope sediment transport.

2 | MATERIALS AND METHODS

2.1 | Indoor simulated scouring experiments

Soil with obvious differences in physical and chemical properties can help reduce the uncertainty of composite tracer identification. Therefore, three soils characterized by different organic matter content and particle size composition were selected as experimental source soils. These source soils come from various regions in China, they are namely black soil (Alfisols) from Shangganling, Heilongjiang Province, Lou soil (Anthrosols) from Yangling, Shaanxi Province, and loess (Entisols) from Mizhi, Shaanxi Province (Table 1) (Soil Survey Staff, 2010). Soil samples were collected from the topsoil, with a depth of approximately 0.2 m. Through visual observation of the soil colour of the three source soils, the soil colour of the black soil with high organic matter content was black-brown, which was in sharp contrast to the colour of the other two source soils. The loess collected on the slope is mainly of the Malan variety, which is light yellow in colour; Lou soil is affected by long-term artificial tillage, fertilization and irrigation, and its colour is grey-brown.

Indoor simulated scouring experiments were conducted to simulate sediment sorting (particle sorting and organic matter enrichment) in the rainfall simulation laboratory of the State Key Laboratory of Soil Erosion and Dryland Farming on the Loess Plateau, Yangling, China. The experimental equipment consists of two parts: an inflow supply device and an experimental flume (Figure 1) (Yang et al., 2022). The inflow supply device is composed of a peristaltic pump, water pipes, a water tank and three steady flow sections. The main role of the peristaltic pump is to accurately deliver and control the flow discharge. The steady flow section is a flume made of aluminium alloy. The experimental flume consists of three flumes with dimensions of 2 m long, 0.2 m wide and 0.15 m high. The bottom of each flume is distributed with some small circular holes whose function is to remove excess water. To adjust and control the experimental slope, we fixed the experimental flume onto a movable steel frame. The slope of this frame varies from 0 to 30° with a variation interval of 5°.

According to the pre-experimental results, two flow levels (1.3 and 1.8 L/min) were selected in the current study. Three experimental

TABLE 1 Basic characterization of the three source soils used in this research

Source soil	Location	Bulk density (g/cm^3)	Clay (%)	Silt (%)	Sand (%)	SOM (g/kg)
Black soil	128.97° E, 47.97° N	1.2	21.5	47.0	31.4	67.5
Lou soil	108.07° E, 34.29° N	1.3	20.2	74.6	5.2	4.8
Loess	110.15° E, 37.91° N	1.2	6.2	34.4	59.4	5.2

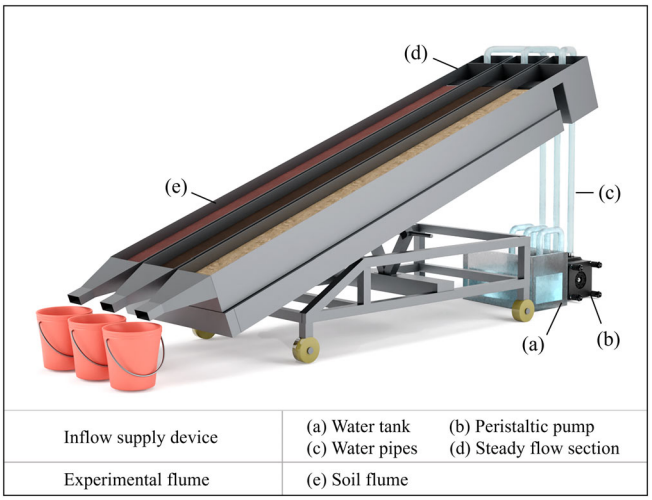

FIGURE 1 Sketch of the simulated scouring experimental device.

slope gradients (10, 15, and 20°) were used to simulate field conditions because the gradient of sloping agricultural land in China is mostly between 10° and 20° (Wang et al., 2019). A total of six scouring experiments with different flow discharges and slope gradients were conducted to observe the responses of sediments with different proportions of sediment sources and to simulate particle sorting in the process of soil transport on the slope (Dai et al., 2022). The specific settings of the flow discharge and slope gradient of these experiments are shown in Table 2.

The experimental source soils collected from the field were air-dried in the laboratory, then crushed and passed through a 10 mm sieve to remove weeds and stones before being filled into the experimental flume. A layer of gauze was packed at the bottom of the flume to ensure good water permeability. The soils were filled in the flume layer by layer to create a filling bulk density consistent with the bulk density of the three experimental soils in the field (Table 1). Once the flumes were filled with the soils, the surface layer of each was slightly raked to ensure uniformity. To reduce the sidewall effect, both sides of the surface were compacted. Before conducting each experiment, the experimental flumes were wetted with a sprinkler until surface flow occurred. The purpose of sprinkling was to keep the soil water content consistent. To prevent tested soil moisture transpiration, the tested soils were covered with permeable gauze which was left for 10 h.

Prior to carrying out each scouring experiment, discharge flow was carefully calibrated. The formal experiment could be started when the discharge flow reached the design flow level. During scouring experiments, stopwatches were used to record the time of runoff, and each experiment took 15 min. The scouring single samples of each experimental flume were collected in three buckets with a volume of approximately 5 L throughout the scouring process. Meanwhile, additional scouring samples were collected by using 220 mL plastic cups at 1, 4 and 8 min, and then used for measuring particle size distribution.

TABLE 2 Flow and slope combination of six scouring experiments

Scouring times	Flow level (L/min)	Slope (°)
1	1.3	10
2	1.8	10
3	1.3	15
4	1.8	15
5	1.3	20
6	1.8	20

2.2 | Sample collection

The study involved three types of samples, namely three source soil samples, scouring single samples and mixtures. Source soil samples involved the collection of 10 duplicate samples from each source soil. A total of 18 scouring single samples were collected in 6 scouring experiments. All scouring single samples were air-dried at 40°C and weighed by using a two-decimal place balance.

We formulated three types of mixtures, namely reference samples, scouring mixtures and artificial mixtures, respectively. A total of 45 reference samples of different ratios for calibrating spectroscopic models were created using three source soils. The contribution of each source soil in reference samples, shown in Figure 2, ranged from 0% to 100%, with an increment of 12.5%. Three scouring single samples from each scouring experiment were mixed with water to form scouring mixtures with known source ratios (Water is used to ensure the uniformity of scouring mixtures), and a total of 6 kinds of scouring mixtures were obtained (Table 3). For each scouring mixture, 4 duplicate samples were collected by using the method of quartering. Artificial mixtures were obtained by mixing three source soils, and the mixing ratios and number of samples were consistent with those of the scouring mixtures.

2.3 | Laboratory measurements

All samples were gently disaggregated using a pestle and mortar and sieved to 2 mm. Source soils and scouring single samples were analysed for soil organic matter (SOM) content and particle size distribution. The particle size distribution of samples was measured by using a Malvern Mastersizer 2000 (Malvern Instruments Ltd, Worcestershire, UK) instrument (Callesen et al., 2018). The tested samples first needed to have their SOM and carbonate removed with a hydrogen peroxide and hydrochloric acid solution, then they had sodium hexametaphosphate added for chemical dispersion, and finally ultrasonic dispersion before measurement. The potassium dichromate oxidation-external heating method was used to measure SOM content. To avoid the influence of large particles on the spectral results during the measurement process, all samples were uniformly ground to 150 μm. Samples were then oven-dried at 45°C for 8 h before the spectral analysis.

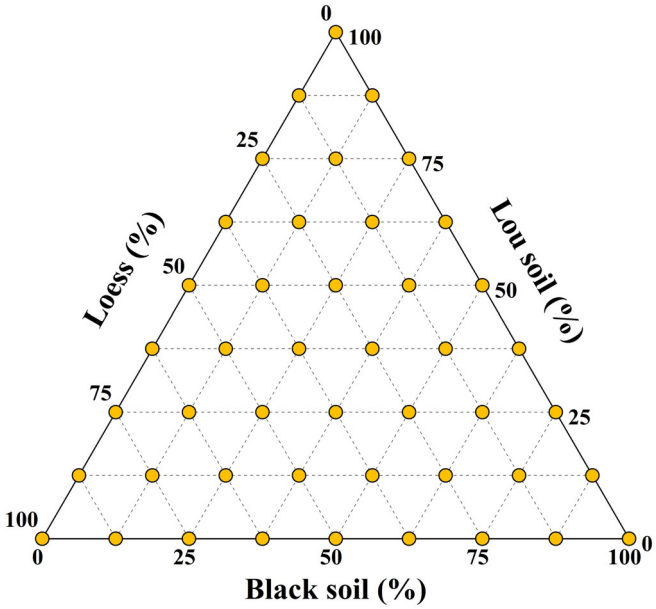

FIGURE 2 Ternary diagram with 45 reference samples with different sediment source ratios. Each point represents a mixing ratio.

TABLE 3 The contributions of sources in six scouring experiments

Experiment number	Black soil (%)	Lou soil (%)	Loess (%)
1	31.00	28.00	41.00
2	6.00	36.00	58.00
3	17.00	26.00	57.00
4	8.00	16.00	76.00
5	20.00	36.00	44.00
6	23.00	40.00	37.00

Visible reflectance spectroscopy was measured in the range of 360–750 nm using a CS-820 spectrophotometer (CS-820, China) with a resolution of 10 nm. The measurements were taken with a D65 standard illuminant and 10° angle observer, including the specular component. A white and black calibration was applied to the device before the samples were measured. During the measurement process, firstly, cuvettes containing the samples were fixed on the measuring pores (6 mm); then the measurement button was clicked to complete the measurement; finally, the final measurement results were calculated as the average value of the three measurements. Considering the possible heterogeneity of the soil and the small measuring area, three separate replicates were performed for each sample (Legout et al., 2013). Meanwhile, nineteen colour parameters (19) were also obtained from VIS spectroscopy by using different colorimetry models (Viscarra Rossel et al., 2006). Colour QC 2 software (CS-820, China) was used to calculate these parameters. All the colour parameters used in the current study are shown in Table 4.

Near-infrared spectroscopy (12000–4000 cm^{-1}) measurements were recorded in diffuse reflectance mode using a Bruker MPA FT-NIR spectrometer (Bruker, USA) with gold-plated reflection

TABLE 4 Nineteen colour parameters calculated using Colour QC 2 software

Colour space model	Colour parameter	Parameter abbreviation
RGB	red	R
	green	G
	blue	B
CIE XYZ	virtual component X	X
	brightness	Y
	virtual component Z	Z
CIE xyY	chromatic coordinate x	x
	chromatic coordinate y	y
CIE Luv	metric lightness function	L
	chromatic coordinate opponent red–green scales	u*
	chromatic coordinate opponent blue–yellow scales	v*
CIE Lab	chromatic coordinate opponent red–green scales	a*
	chromatic coordinate opponent blue–yellow scales	b*
CIE Lch	CIE hue	c
	CIE chroma	h
Decorrelated RGB	hue	H_{RGB}
	light intensity	I_{RGB}
	chromatic information	S_{RGB}
Index	redness index	RI

accessories. Each NIR spectral data was the average value of the 64 scans at a resolution of 8 cm^{-1}. In order to deduct the influence of the spectrometer itself on the sample spectrum, background measurement was an essential step before soil sample measurement. After measuring, OPUS software (Bruker, USA) provided by the spectrometer producers was used to collect and process sample spectral data.

A Thermo Nicolet iS50 infrared spectrometer (Thermo Nicolet, USA) was used to measure mid-infrared spectroscopy in diffuse reflectance mode. The spectroscopy can range from 4000 to 400 cm^{-1} in a resolution of 4 cm^{-1} with 64 co-added scans of each spectroscopy. The scraper equipped with the instrument was used to create a smooth surface of the measured samples. The range of 2400–2300 cm^{-1} from the analysis needed to be removed to avoid CO_2 effects (Tiecher et al., 2017). OMNIC software (Thermo Nicolet, USA) was used to collect the spectral data.

2.4 | Sediment source discrimination and apportionment

2.4.1 | Spectroscopy approach

Spectroscopic data are composed of a set of continuous variables. Therefore, we performed a series of statistical analyses proposed by

Poulenard et al. (2009) to differ from conventional fingerprinting methods. Specifically, the steps of the method based on spectroscopic data are as follows. First, a principal component analysis (PCA) was performed to reduce the dimension of spectral data of the three sediment source samples. Then a linear discriminant analysis (LDA), based on maximizing the distances between sediment source groups and minimizing the distances within sediment source groups, was conducted by using the scores generated by the PCA as input variables to evaluate the discrimination power of the spectroscopic tracers.

To calibrate spectral models, three commonly-used multivariate methods were combined, with 45 reference samples with different ratios (Figure 2). These multivariate methods are partial least squares regression (PLSR), principal component regression (PCR) and support vector machines (SVM), respectively. The spectral models were verified by using the leave-one-out cross validation (LOOCV) method. Root mean square error (RMSE) and coefficient of determination (R^2) were selected to evaluate model prediction performance [Equation (1) and (2)]. Then, the differences in RMSE and R^2 values of different spectral models were compared. And the optimal model was defined as the spectral model with the lowest RMSE and highest R^2 value in the condition of the same sediment source and spectral range. In short, nine independent spectral models were established to calculate the sediment contribution of three sediment sources in this study.

$$R^2 = 1 - \frac{\sum_{i=1}^{n}(y_i - \widehat{y}_i)^2}{\sum_{i=1}^{n}(y_i - \overline{y})^2} \tag{1}$$

$$RMSE = \sqrt{\frac{1}{n}\sum_{i=1}^{n}(y - \widehat{y}_i)^2} \tag{2}$$

Where n is the number of sources, y_i is the measured value, $\widehat{y}_i$ is the predicted value, $\overline{y}$ is the mean value.

2.4.2 | Conventional fingerprinting methods–colour parameters

The conventional fingerprinting method based on colour parameters was performed for this research. This method mainly consists of two parts: construction of the best composite fingerprints and calculation of the relative contribution of sediment source. Firstly, the range test was used to examine the conservation of tracers. The purpose of this test was to ensure that tracer concentrations in sediments were located between sources with the highest and lowest concentrations. Then, a two-step procedure was performed to construct the composite fingerprints with the best discriminative ability (Collins, 1997). The first step was to carry out a nonparametric Kruskal-Wallis H (KW-H) test to select individual fingerprint property that can distinguish between sediment sources. Subsequently, a stepwise discriminant function analysis (DFA) was performed to determine an optimal source fingerprint combination by minimizing Wilk's lambda. Subsequently, the multivariate mixing linear (MML) model and MixSIAR model were used to calculate the relative contribution of each sediment source to the target sediments. The MML model (Walling, 2005) is the most widely used model, and the equation is shown in Equation (3). The genetic algorithm (MML-GA) (Chen et al., 2016) was selected to calculate the MML model. Matrix Laboratory software (Matlab) was used to perform the genetic algorithm. The algorithm searched for the best source contribution rate of the target sediment through adaptive iteration (Collins et al., 2010; Dai et al., 2022). The advantage of GA is that it can search for the optimal result globally. In addition, 2500 iterations of Monte Carlo techniques were used as an alternative to traditional random sampling methods for solving unmixing model in this research. When R value is the minimum value. P_s value is the relative contribution value of the sediment source to the target sediment.

$$R = \sum_{i=1}^{m}\left\{\left[C_i - \left(\sum_{s=i}^{n} P_s C_{si}\right)\right]/C_i\right\}^2 \tag{3}$$

Where n represents the number of sediment sources. m is the number of the tracer. C_i is the tracer i concentration in the target sediment sample. C_{si} is tracer i concentration of sediment source s. P_s is the relative contribution of the sediment source s. Meanwhile, two limitations [Equation (4) and Equation (5)] need to be considered when applying Equation (3):

$$0 \le P_s \le 1 \tag{4}$$

$$\sum_{s=1}^{n} P_s = 1 \tag{5}$$

The MixSIAR model was introduced into sediment source research from the ecological field (Stock et al., 2018). This method used prior information to calculate the probability distribution of the relative contribution of each sediment source. According to Bayesian theory, the posterior probability distribution of the relative contribution of different sediment sources is the direct proportion to the prior probability based on prior information as shown in Equation (6):

$$P(f_q|data) = \frac{L(data|p(f_q))}{\sum L(data|f_q) \times p(f_q)} \tag{6}$$

Where $L(data|f_q)$ represents the likelihood function of the given data f_q. $p(f_q)$ is the prior probability based on prior information. f_q represents the relative contribution of each sediment source. In addition, the likelihood function is obtained by Equation (7):

$$L(x|\widehat{\mu}_j, \widehat{\sigma}_j) = \prod_{k=1}^{n}\prod_{j=1}^{n}\left[\frac{1}{\widehat{\sigma}_j \times \sqrt{2 \times \pi}} \times \exp\left(-\frac{(X_{kj} - \widehat{\mu}_j)^2}{2 \times \widehat{\sigma}^2}\right)\right] \tag{7}$$

where $\widehat{\mu}_j$ and $\widehat{\sigma}_j$ represent the mean and standard deviation values in the jth tracer concentration in the target sediment, respectively. X_{kj} is the jth tracer of the kth target sediment sample.

The actual calculation of the MixSIAR model is implemented on R using the MixSIAR package (Stock et al., 2018). Firstly, the three sets of files of Mixture (the colour parameter data of the target sediment), Source (mean and standard deviation value of the source colour parameters), and TDF (discrimination factor data) are loaded into

the model; then the Markov Chain Monte Carlo (MCMC) run length is set to normal (chain Length = 100 000, burn = 50 000, thin = 50, chains = 3); finally, the mean value of each source obtained by running the MixSIAR model is the contribution rate of the source to the target sediment.

2.5 | Evaluating indicators of sediment sorting

The enrichment ratio was used to evaluate the particle sorting degree of scouring single samples (Martínez-Mena et al., 2002). The enrichment ratio of particle size could be calculated by Equation (8):

$$ER_{PS} = \frac{PS_{scouring}}{PS_{source}} \quad (8)$$

Where PS_{source} is the particle size (%) in the three source soils and $PS_{scouring}$ is the particle size in the scouring single samples. ER_{PS} represents the enrichment ratio of particle size in the scouring process.

The enrichment ratio of soil organic matter [Equation (9)] was used to assess the enrichment degree of the organic matter content of scouring single samples:

$$ER_{OM} = \frac{OM_{scouring}}{OM_{source}} \quad (9)$$

Where OM_{source} is the organic matter content (g/kg) in the three source soils and $OM_{scouring}$ is the organic matter content (g/kg) in the scouring single samples. ER_{OM} represents the enrichment ratio of organic matter content in the scouring process.

2.6 | Accuracy of optical fingerprints

The accuracy of fingerprinting results by using different optical fingerprints was tested based on mean absolute error (MAE) [Equation (10)] for target sediments:

$$MAE = \frac{\sum_{j=1}^{n} |X_j - Y_j|}{n} \quad (10)$$

where X_j is the actual percentage of source in target samples, Y_j is the calculated contribution of source (j); n is the number of sediment sources.

3 | RESULTS

3.1 | Characterization of source soils and target sediments

Figure 3 displays the mean reflectance spectroscopy in VIS, NIR and MIR ranges for three sediment sources and two target sediments (scouring mixture and artificial mixtures). These spectroscopies reflect the information on organic matter and minerals in soil and sediment (Madari et al., 2006). The positions of the characteristic peaks of the

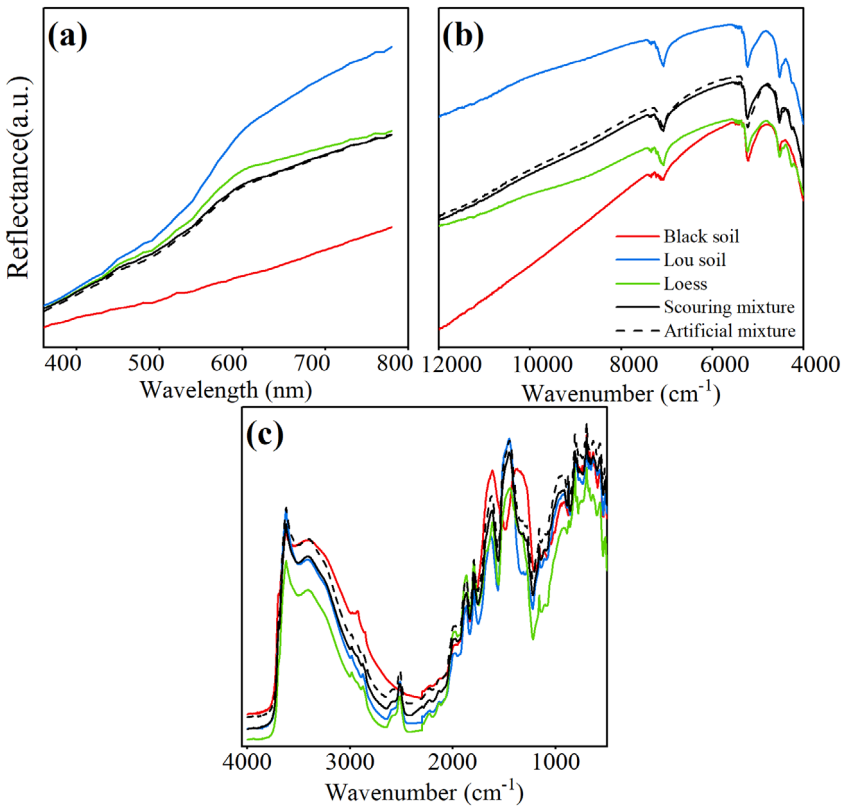

FIGURE 3 Mean VIS (a), NIR (b) and MIR (c) reflectance spectroscopy of the three sediment sources and two target sediments.

three sediment sources in VIS and NIR spectroscopic ranges are roughly the same, but the reflection values are significantly different. In the MIR spectral bands, the characteristic peak positions of Lou soil and loess are the same, both with an absorption peak (2515, 1795, 1450 and 879 cm^{-1}) related to carbonate, but their absorbance is different (Andersen & Brecevic, 1991; Ni et al., 2019). The absorption peak position and absorbance of black soil are different from those of the other two sources. Comparing the positions and values of the characteristic peaks of the mixture and sediment source spectra, the characteristic peaks of the two target sediments (artificial mixtures and scouring mixtures) and the source samples have the same positions, and the absorptions or reflection values of the target sediments are between the three source samples. The comparison results show the conservation of spectral features.

Table 5 shows the colour parameters concentrations and coefficient of variations (CV) of three sediment sources and two target sediments. Among the 19 colour parameters, the CV of the H_{RGB} parameter was between 8.63% and 20.07%, indicating that this parameter varied largely from three sediment sources and was removed in the following analysis. The CVs of the remaining 18 colour parameters were less than 5%. Additionally, the concentrations of 18 colour parameters between sediment sources and target sediments were compared to verify the conservative behaviour of colour parameters. The results showed that only the h parameter was excluded due to the maximum value of this parameter of the target sediments exceeded that of these sediment sources, while other parameters have passed the range test.

The results of particle size distribution and SOM in three source soils are shown in Table 1. The SOM content of black soil was significantly higher than that of Lou soil and loess, reaching 67.5 g/kg ($p < 0.05$). Lou soil and loess were characterized by low values of SOM and no significant differences between them. The particle size distribution was also significantly different between the three source soils.

3.2 | Discriminant results and optimal tracers

The PCA results showed that the first two, two and seven principal components explained more than 99% of the variation in VIS, NIR and MIR spectroscopy, respectively. Subsequently, LDA was performed by using these principal components. The LDA results showed that VIS, NIR and MIR spectroscopic data could effectively distinguish these experimental source soils. Nine independent optimal predictive models were selected by comparing the differences in RMSE and R^2 (Table 6). The performance of these models was excellent with R^2 close to 1. Moreover, the values of RMSE were lower than 0.12 showing that these models had good predictive performance.

In this study, 17 colour parameters were selected as potential tracers. The KW-H test was used to exclude tracers with no significant difference between sediment sources (Table 7), the results indicated that all tracers passed the test. Then the DFA results determined that the optimal combination of tracers obtained could correctly classify the three sources 99% (Table 7).

TABLE 5 Minimum (min), maximum (max) and coefficient of variation (CV) of 19 colour parameters of three sediment sources and two target sediments

Sediment/source	Index	X	Y	Z	R	G	B	L	a*	b*	c	h	x	y	u*	v*	RI	H_{RGB}	I_{RGB}	S_{RGB}
Black soil	min	16.78	17.30	15.81	122.91	113.06	105.09	48.64	2.07	5.80	6.17	69.49	0.3360	0.3470	5.99	7.99	0.5405	0.3957	113.68	8.75
	max	17.83	18.38	16.69	126.85	115.99	107.71	49.95	2.22	6.16	6.53	70.57	0.3370	0.3470	6.28	8.51	0.6200	0.6476	116.85	9.57
	CV	1.65%	1.66%	1.50%	0.83%	0.80%	0.74%	0.73%	2.11%	1.97%	1.92%	0.45%	0.14%	0.00%	1.82%	2.01%	3.82%	20.07%	0.78%	2.41%
Lou soil	min	32.46	32.15	23.45	176.80	148.24	124.13	63.47	7.14	16.40	17.91	65.98	0.3680	0.3650	19.69	21.49	0.1602	1.1199	149.84	26.01
	max	33.17	32.88	24.05	178.78	149.87	125.78	64.06	7.37	16.70	18.22	66.52	0.3690	0.3650	20.06	21.89	0.1683	1.4429	151.47	26.66
	CV	0.81%	0.87%	0.94%	0.38%	0.46%	0.48%	0.36%	0.95%	0.54%	0.54%	0.28%	0.14%	0.00%	0.60%	0.55%	1.91%	8.63%	0.41%	0.83%
Loess	min	27.45	27.69	21.61	160.37	139.45	120.19	59.61	4.84	13.04	13.91	69.20	0.3570	0.3600	14.23	17.44	0.2004	0.3444	140.00	19.93
	max	28.96	29.22	22.79	164.32	143.03	123.48	60.98	5.00	13.39	14.27	69.76	0.3580	0.3610	14.62	17.94	0.2247	0.5074	143.61	20.58
	CV	1.54%	1.57%	1.63%	0.70%	0.77%	0.82%	0.66%	1.25%	0.82%	0.83%	0.25%	0.15%	0.15%	0.98%	0.85%	3.36%	15.32%	0.75%	0.94%
Scouring mixture	min	24.89	25.25	20.57	152.40	134.57	118.56	57.32	3.95	10.79	11.50	67.87	0.3510	0.3560	11.64	14.59	0.2052	0.2300	135.18	16.48
	max	28.81	29.03	23.43	164.42	143.10	125.92	60.81	5.32	13.45	14.44	71.01	0.3590	0.3610	15.09	17.93	0.2733	0.7975	144.03	20.81
Artificial mixture	min	24.86	25.34	20.76	151.69	135.01	119.10	57.41	3.63	10.76	11.48	65.97	0.3500	0.3560	11.20	14.50	0.2051	0.1525	135.29	16.30
	max	28.85	29.01	22.55	165.16	142.69	123.30	60.79	5.79	13.63	14.64	71.56	0.3590	0.3610	15.57	18.16	0.2705	1.1725	143.60	21.11

TABLE 6 R^2 and RMSE values of nine optimal models selected in VIS, NIR and MIR spectroscopic ranges

Spectral range	Source soil	Model	R^2	RMSE
VIS	Black soil	PCR	0.941	0.048
	Lou soil	SVMR	0.919	0.079
	Loess	SVMR	0.841	0.113
NIR	Black soil	PLSR	0.980	0.047
	Lou soil	PLSR	0.964	0.054
	Loess	PLSR	0.947	0.065
MIR	Black soil	PLSR	0.986	0.036
	Lou soil	SVMR	0.966	0.052
	Loess	SVMR	0.960	0.056

TABLE 7 Results of failed KW-H test and optimal tracers by DFA for colour parameters in scouring mixtures and artificial mixtures

Target sediment type	Scouring mixtures	Artificial mixtures
Colour parameter that failed KW-H test	—	—
Optimal colour parameters by DFA	C, y, u*	C, y, u*

3.3 | Source apportionments of four optical fingerprints

The MAE values of fingerprinting results of two target sediments (scouring mixtures and artificial mixtures) by using four optical properties (VIS, NIR, MIR and colour parameter) are shown in Figure 4 and Figure 5. For the VIS, NIR and MIR spectroscopic tracers, the MAE values of three spectroscopic ranges were lower than 12%, indicating that spectroscopic tracers could provide high prediction accuracy in the condition of artificial mixing and indoor scouring. For colour parameters, MAE values ranged from 8.98% to 25.33% in scouring mixtures and from 8.11% to 18.56% in artificial mixtures, which were significantly higher than those of VIS, NIR and MIR spectroscopy.

In addition, we compared the difference in prediction accuracy of VIS, NIR and MIR spectroscopy by using MAE values. The MIR spectroscopy exhibited the lowest MAE values of fingerprinting results with mean values of 2.45% and 3.16% in two target sediments, indicating that MIR spectroscopic tracers could more accurately predict target sediments compared with VIS and NIR spectrums. This was followed by VIS spectroscopic tracer ranging from 3.41% to 9.16%. The highest MAE values ($MAE_{scouring} = 7.00\%$ and $MAE_{artificial} = 8.83\%$) and variations ($SD_{scouring} = 1.98\%$ and $SD_{artificial} = 2.08\%$) in three spectroscopic ranges were acquired by using NIR spectroscopy.

3.4 | The influence of sediment sorting on fingerprinting accuracy

Figure 6 shows the results of particle size distribution and enrichment ratio (ER_{PS}) of 18 scouring single samples. The results indicated that each scouring single sample experienced different degrees of particle sorting. The smallest particle sorting occurred in loess scouring single samples with a variation of enrichment ratio of 0.94–1.21. The particle sorting ability of black scouring single samples with ER_{PS} values from 0.85 to 1.22 was slightly stronger than that of loess scouring single samples. The enrichment ratio of most Lou scouring single samples ranged from 0.84 to 1.03. Though some of the high values of enrichment ratios with 1.72, 1.85, 1.96, 2.21 and 2.83 occurred in Lou scouring single samples, they were all sand fractions with a very small proportion (volume percentage: 8.88%–14.60%). Black scouring single samples had the lowest variation of enrichment ratio of organic matter of 0.89–1.04 and the highest organic matter content (mean = 66.66±3.79 g/kg). In contrast, although the enrichment ratio of SOM of Lou scouring single samples and loess scouring single samples varied greatly ($ER_{OM} = 0.67–1.07$), their SOM contents were significantly lower than those of black scouring single samples.

To evaluate the influence of particle size and organic matter on the accuracy of four optical properties, the fingerprinting results of scouring mixtures and artificial mixtures (Figure 7) were compared. For fingerprinting results of scouring mixtures using VIS, NIR and MIR spectroscopy and colour parameters, the MAE values were 5.50%, 7.00%, 2.45% and 16.83%, with a mean value of 7.95%. The MAE values of artificial mixtures by these tracers were 5.74%, 8.83%, 3.16% and 15.05%, with a mean value of 8.20%. In general, the mean MAE values of scouring mixtures were consistent with artificial mixtures.

4 | DISCUSSION

4.1 | Prediction accuracy of different optical features

Our results confirmed that the source apportionments were sensitive to the selection of spectroscopic ranges, in agreement with the findings of previous studies (Farias Amorim et al., 2021; Tiecher et al., 2021). This may be attributed to differences in soil absorption characteristics in VIS, NIR and MIR wave bands. In this study, the MIR spectroscopic tracer showed the highest prediction accuracy compared with the other two spectra (Figure 4 and Figure 5). High prediction accuracy from MIR spectroscopy also was observed in several other studies (Chapkanski et al., 2020; Poulenard et al., 2009). This result may be attributed to soil absorption characteristics in the MIR wave bands. This spectrum not only had obvious absorption features but also carried a larger amount of soil information compared with VIS and NIR spectrum. Therefore, the sensitivity of MIR spectra to organic compounds is higher than that of VIS and NIR spectroscopy (Rossel & Behrens, 2010; Tiecher et al., 2021). MIR spectroscopy can identify C-H, C-O, and C-N functional groups that dominate soil organic matter (Knox et al., 2015; Soriano-Disla et al., 2014). However, the high dependence of MIR spectroscopy on the organic matter can also lead to an overestimation of the surface source of sediments (Evrard et al., 2013; Tiecher et al., 2017).

Colour parameters and VIS spectroscopy were characteristic parameters of visible absorption in soil samples. In our results, a

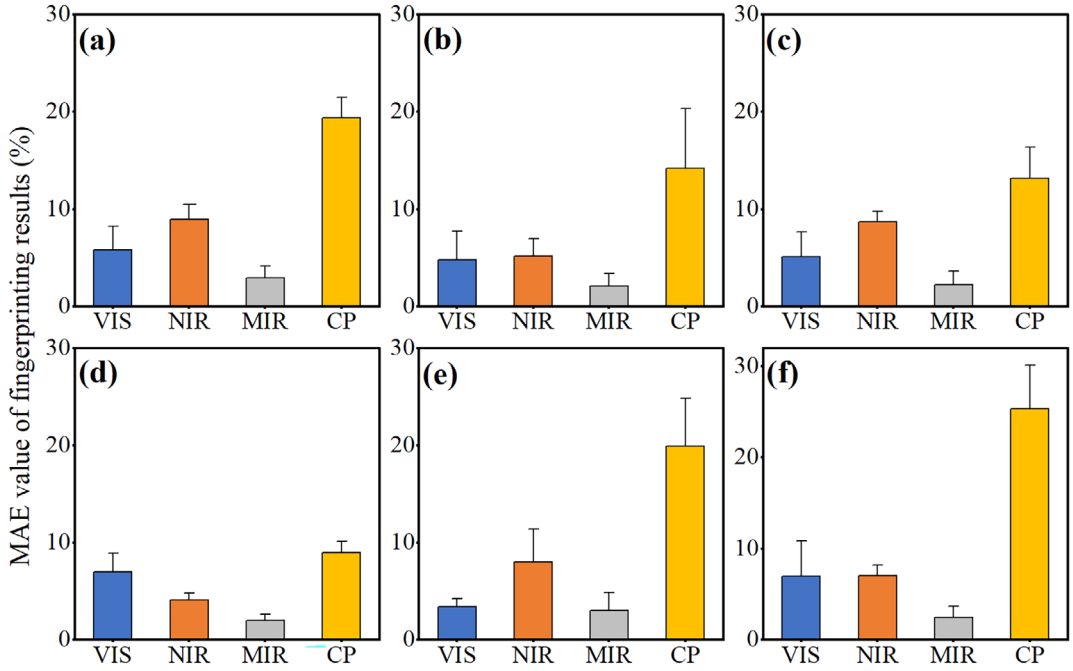

FIGURE 4 The mean absolute error (MAE) of fingerprinting results for VIS, NIR, MIR spectroscopy and colour parameters (CP) in six scouring experiments (a-f represents the first to sixth scouring mixtures respectively).

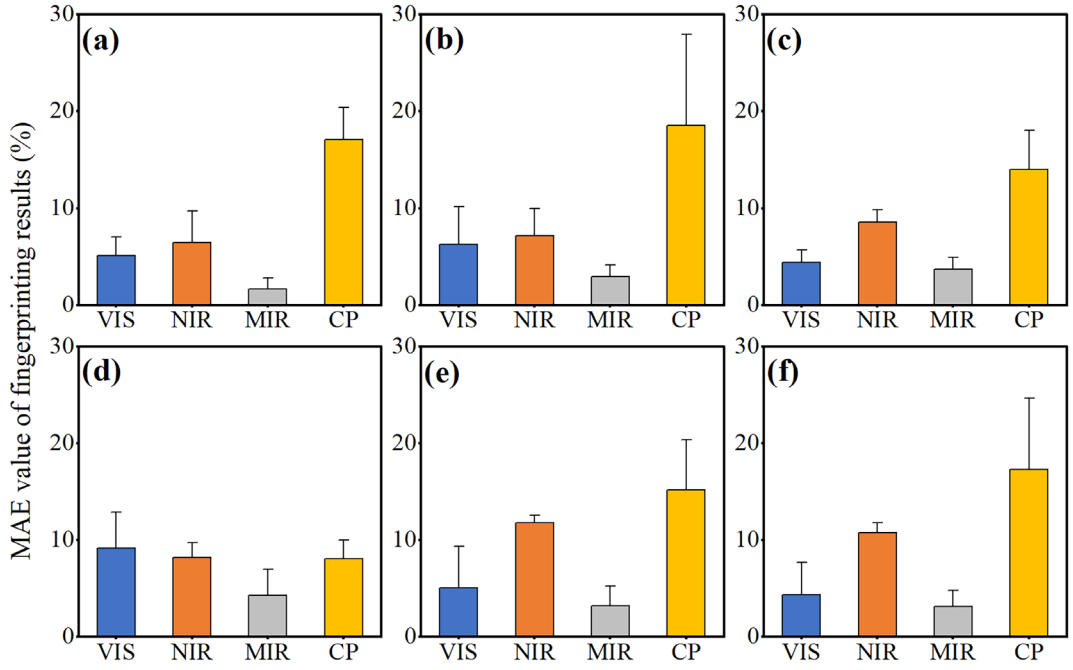

FIGURE 5 The mean absolute error (MAE) of fingerprinting results for VIS, NIR, MIR spectroscopy and colour parameters (CP) in six artificial mixtures (a-f represents the six designed ratio of artificial mixtures respectively).

significant difference was found between colour parameters and VIS spectroscopy (Figure 4 and Figure 5), which was also consistent with that of Tiecher et al. (2015). There are two possible explanations for this difference. First, fingerprinting results of target sediments were obtained by using small numbers of colour parameter tracers selected by discriminant analysis. In contrast, VIS spectral models were established to use 45 reference samples containing different ratios of sediment source (Gaspar et al., 2019; Ni et al., 2019). Then, the colour parameters were only calculated from a part range of the VIS spectra, which might lead to the loss of information and affect the accuracy of

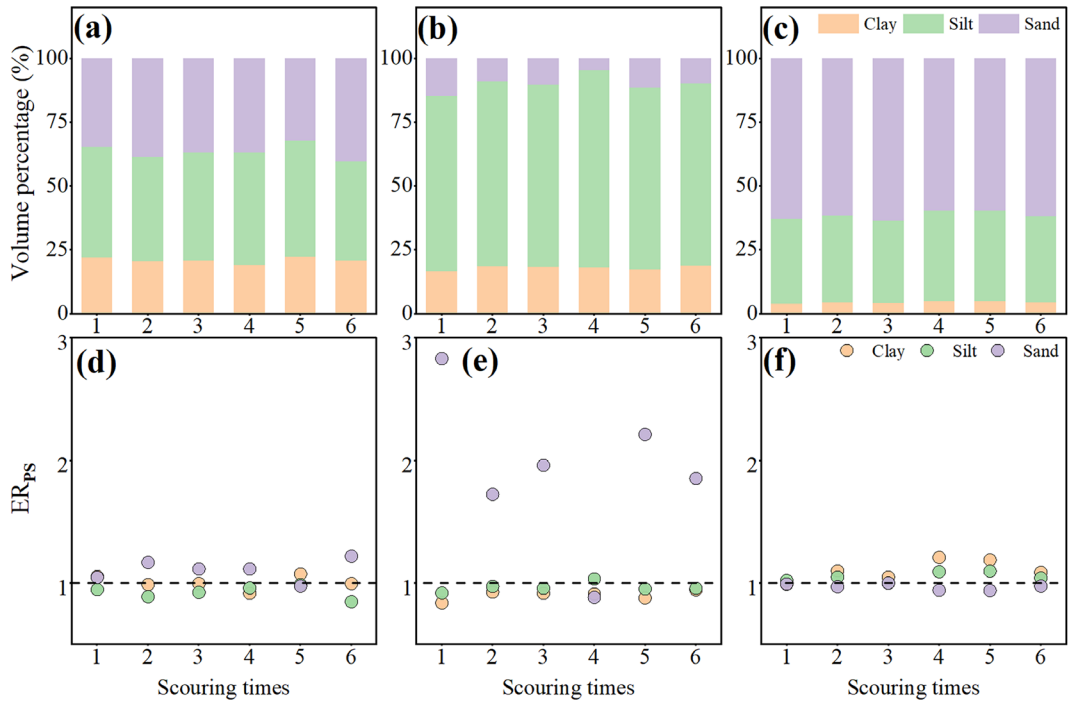

FIGURE 6 Volume percentage (a-c) and enrichment ratio of particle size (ER_{PS}) (d-f) of three scouring single samples in six scouring experiments (a, d represent black scouring single samples; b, e represent Lou scouring single samples; c, f represent loess scouring single samples).

the fingerprinting results (Sellier et al., 2021; Tiecher et al., 2015). To further explore the applicability of colour parameter tracers, 42 reference samples (excluding 3 single source samples; the details of reference samples can be seen in Section 2.2 of the manuscript) were divided into two groups, namely two source reference samples (samples were mixed from two source soils) and three source reference samples (samples were mixed from three source soils). A low MAE value of 4.81% was obtained in two source reference samples, while a high MAE value of 22.67% was obtained in three source reference samples (Figure 8). A possible explanation for this might be that an increase in the number of sources may increase the complexity of the running of the model (Vale et al., 2016, 2022). The main reason for reduced prediction accuracy as the number of sources increases is that these sources may have similar colour characteristics. In our study, the differences in colour characteristics between Lou soil and loess were significantly lower than those between black soil and Lou soil or loess in three source reference samples. Most of the colour parameters are related to each other and can show similar values in Lou soil and loess, which may lead to a decline in the ability to distinguish Lou soil and loess in the prediction process of three source reference samples, thus reducing the prediction accuracy (Collins et al., 2020).

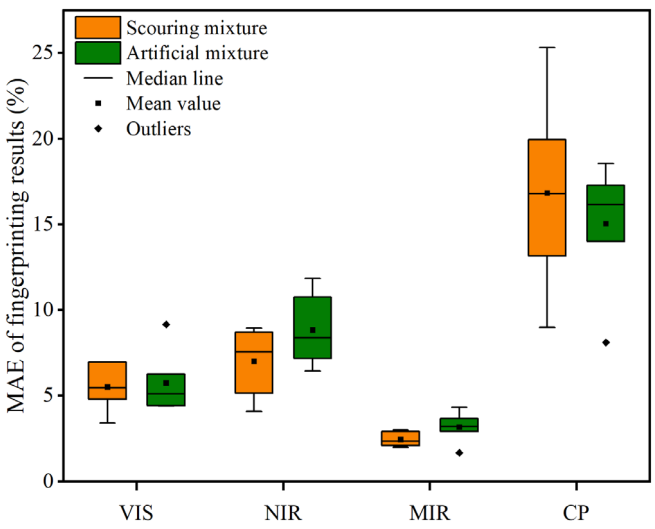

FIGURE 7 The mean absolute error (MAE) of fingerprinting results for two target sediments (scouring mixtures and artificial mixtures) by using VIS, NIR, MIR spectroscopy and colour parameters (CP).

4.2 | Effect of sediment sorting on optical fingerprinting

Particle size and organic matter are key factors affecting the accuracy of sediment source fingerprinting results (Laceby et al., 2017). They affect conservative behaviour by changing the concentration distribution of soil components and particle size distribution (Koiter et al., 2015), and they then affect the source assignment results (Gaspar et al., 2022). In this study, we found only minor differences between artificial mixtures and scouring mixtures that were subjected to particle sorting and organic matter enrichment (Figure 7). This may be attributed to slight particle sorting and organic matter enrichment.

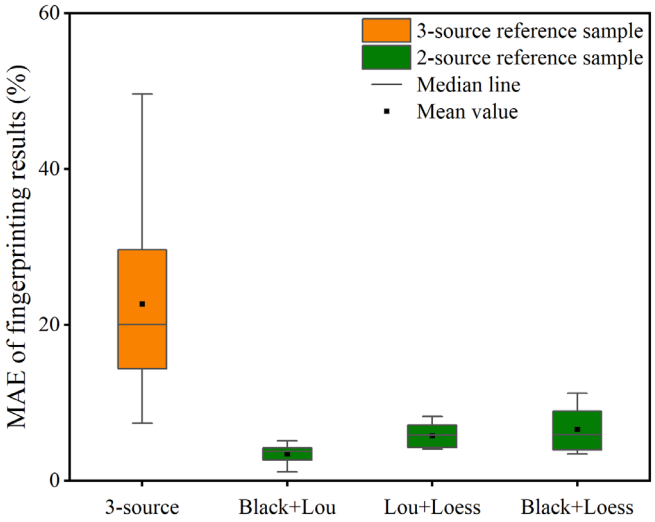

FIGURE 8 The mean absolute error (MAE) of fingerprinting results for 42 reference samples (3-source reference samples and 2-source reference samples) by using colour parameters. 3-source reference samples were mixed from three source soils (black soil, Lou soil and loess); 2-source reference samples were mixed from two source soils (black soil+ Lou soil; Lou soil+ loess; black soil+ loess).

The research of Pulley and Rowntree (2016) showed that the results were affected only when the content of organic matter was increased to the proportion of more than 30% of the mass of matter during the tracing study of obvious differences between the source soils. In our study the organic matter content of these scouring mixtures ranged from 0.75% to 2.16%. In addition, although the scouring mixtures had particle sorting with the highest value of 2.83, the particle size enrichment ratios of most of the samples ranged from 0.84 to 1.22 (Figure 6) (Han et al., 2019). The sand fraction of the 4 scouring single samples with only Lou soil exceeded 1.5 and this fraction did not contribute much to the whole sample. Therefore, it is necessary to study the influence of stronger particle size sorting on the accuracy of sediment source fingerprinting results in the future.

5 | CONCLUSIONS

In this paper, artificial mixing and simulated scouring experiments were designed to verify the accuracy of fingerprinting results using 19 colour parameters with conventional method and three spectral ranges (VIS, NIR and MIR spectroscopy) with multivariate methods. In general, VIS, NIR and MIR spectroscopic tracers presented high accuracy in sediment source identification. Among the tested three spectroscopic features, the lowest MAE values of fingerprinting results were obtained by using MIR spectroscopy. Furthermore, colour parameters were less reliable than spectroscopic methods, especially to estimate sediments with multiple sources.

Among the two target sediments (scouring and artificial mixtures) tested in this study, similar MAE values indicated that the accuracy of fingerprinting results was not affected by slight particle sorting and organic matter enrichment. Future work is needed to fully understand the implications of greater particle sorting and organic matter enrichment in the accuracy of fingerprinting results by using spectroscopic tracers and to discuss the applicability of colour parameter tracers in tested soils with low colour differences. In short, the results of this study can be used to deepen the understanding of fingerprinting results obtained by optical features and provide a reference for the application of optical features in sediment source identification.

ACKNOWLEDGEMENTS

This work was supported by the National Natural Science Foundation of China (42107361, 42177335, and 41930755) and the Fundamental Research Funds for the Central Universities (2022HXZX002 and 2452020206).

CONFLICT OF INTEREST STATEMENT

The authors declare that they have no known competing financial interests or personal relationships that could have appeared to influence the work reported in this paper.

DATA AVAILABILITY STATEMENT

Research data are not shared.

ORCID

Lingshan Ni https://orcid.org/0000-0002-6462-9110
Nufang Fang https://orcid.org/0000-0001-8157-0256
Zhihua Shi https://orcid.org/0000-0002-6961-1518

REFERENCES

Amundson, R., Berhe, A. A., Hopmans, J. W., Olson, C., Sztein, A. E., & Sparks, D. L. (2015). Soil and human security in the 21st century. *Science*, *348*(6235), 1261071. https://doi.org/10.1126/science.1261071

Andersen, F. A., & Brecevic, L. (1991). Infrared spectra of amorphous and crystalline calcium carbonate. *Acta Chemica Scandinavica*, *45*(10), 1018–1024. https://doi.org/10.3891/acta.chem.scand.45-1018

Callesen, I., Keck, H., & Andersen, T. J. (2018). Particle size distribution in soils and marine sediments by laser diffraction using Malvern Mastersizer 2000—method uncertainty including the effect of hydrogen peroxide pretreatment. *Journal of Soils and Sediments*, *18*(7), 2500–2510. https://doi.org/10.1007/s11368-018-1965-8

Chapkanski, S., Ertlen, D., Rambeau, C., & Schmitt, L. (2020). Provenance discrimination of fine sediments by mid-infrared spectroscopy: Calibration and application to fluvial palaeo-environmental reconstruction. *Sedimentology*, *67*(2), 1114–1134. https://doi.org/10.1111/sed.12678

Chen, F. X., Fang, N. F., & Shi, Z. H. (2016). Using biomarkers as fingerprint properties to identify sediment sources in a small catchment. *Science of The Total Environment*, *557–558*, 123–133. https://doi.org/10.1016/j.scitotenv.2016.03.028

Chen, F. X., Wang, X. Y., Li, X., Wang, J. L., Xie, D. T., Ni, J. P., & Liu, Y. J. (2019). Using the sediment fingerprinting method to identify the sediment sources in small catchments with similar geological conditions. *Agriculture, Ecosystems and Environment*, *286*, 106655. https://doi.org/10.1016/j.agee.2019.106655

Collins, A. L., & Walling, D. E. (2004). Documenting catchment suspended sediment sources: Problems, approaches and prospects. *Progress in Physical Geography*, *28*(2), 159–196. https://doi.org/10.1191/0309133304pp409ra

Collins, A. L., Blackwell, M., Boeckx, P., Chivers, C. A., Emelko, M., Evrard, O., Foster, I., Gellis, A., Gholami, H., Granger, S., Harris, P.,

Horowitz, A. J., Laceby, J. P., Martinez-Carreras, N., Minella, J., Mol, L., Nosrati, K., Pulley, S., Silins, U., … Zhang, Y. (2020). Sediment source fingerprinting: Benchmarking recent outputs, remaining challenges and emerging themes. *Journal of Soils and Sediments*, *20*(12), 4160–4193. https://doi.org/10.1007/s11368-020-02755-4

Collins, A. L., Pulley, S., Foster, I. D. L., Gellis, A., Porto, P., & Horowitz, A. J. (2017). Sediment source fingerprinting as an aid to catchment management: A review of the current state of knowledge and a methodological decision-tree for end-users. *Journal of Environmental Management*, *194*, 86–108. https://doi.org/10.1016/j.jenvman.2016.09.075

Collins, A. L., Walling, D. E., & Leeks, G. J. L. (1997). Source type ascription for fluvial suspended sediment based on a quantitative composite fingerprinting technique. *Catena* Giessen, *29*(1), 1–27. https://doi.org/10.1016/S0341-8162(96)00064-1

Collins, A. L., Williams, L. J., Zhang, Y. S., Marius, M., Dungait, J. A. J., Smallman, D. J., Dixon, E. R., Stringfellow, A., Sear, D. A., Jones, J. I., & Naden, P. S. (2013). Catchment source contributions to the sediment-bound organic matter degrading salmonid spawning gravels in a lowland river, southern England. *Science of the Total Environment*, *456-457*, 181–195. https://doi.org/10.1016/j.scitotenv.2013.03.093

Collins, A. L., Williams, L. J., Zhang, Y. S., Marius, M., Dungait, J. A. J., Smallman, D. J., Dixon, E. R., Stringfellow, A., Sear, D. A., Jones, J. I., & Naden, P. S. (2014). Sources of sediment-bound organic matter infiltrating spawning gravels during the incubation and emergence life stages of salmonids. *Agriculture, Ecosystems and Environment*, *196*, 76–93. https://doi.org/10.1016/j.agee.2014.06.018

Collins, A. L., Zhang, Y., Walling, D. E., Grenfell, S. E., & Smith, P. (2010). Tracing sediment loss from eroding farm tracks using a geochemical fingerprinting procedure combining local and genetic algorithm optimisation. *Science of the Total Environment*, *408*(22), 5461–5471. https://doi.org/10.1016/j.scitotenv.2010.07.066

Dai, W., Chen, D., Li, M. J., Zeng, Y., Ni, L. S., Fang, N. F., & Shi, Z. H. (2022). Validating accuracy of multiple sediment fingerprinting methods. *Land Degradation and Development*, *33*, 3965–3978. https://doi.org/10.1002/ldr.4437

Evrard, O., Batista, P. V. G., Company, J., Dabrin, A., Foucher, A., Frankl, A., García-Comendador, J., Huguet, A., Lake, N., Lizaga, I., Martínez Carreras, N., Navratil, O., Pignol, C., & Sellier, V. (2022). Improving the design and implementation of sediment fingerprinting studies: Summary and outcomes of the TRACING 2021 scientific school. *Journal of Soils and Sediments*, *22*(6), 1648–1661. https://doi.org/10.1007/s11368-022-03203-1

Evrard, O., Laceby, J. P., Ficetola, G. F., Gielly, L., Huon, S., Lefevre, I., Onda, Y., & Poulenard, J. (2019). Environmental DNA provides information on sediment sources: A study in catchments affected by Fukushima radioactive fallout. *Science of the Total Environment*, *665*, 873–881. https://doi.org/10.1016/j.scitotenv.2019.02.191

Evrard, O., Poulenard, J., Némery, J., Ayrault, S., Gratiot, N., Duvert, C., Prat, C., Lefèvre, I., Bonté, P., & Esteves, M. (2013). Tracing sediment sources in a tropical highland catchment of Central Mexico by using conventional and alternative fingerprinting methods. *Hydrological Processes*, *27*(6), 911–922. https://doi.org/10.1002/hyp.9421

Farias Amorim, F., da Silva, Y. J. A. B., Cabral Nascimento, R., da Silva, Y. J. A. B., Tiecher, T., Williams Araújo Do Nascimento, C., Paolo Gomes Minella, J., Zhang, Y., Ram Upadhayay, H., Pulley, S., & Collins, A. L. (2021). Sediment source apportionment using optical property composite signatures in a rural catchment. *Brazil. Catena*, *202*, 105208. https://doi.org/10.1016/j.catena.2021.105208

Gaspar, L., Blake, W. H., Lizaga, I., Latorre, B., & Navas, A. (2022). Particle size effect on geochemical composition of experimental soil mixtures relevant for unmixing modelling. *Geomorphology*, *403*, 108178. https://doi.org/10.1016/j.geomorph.2022.108178

Gaspar, L., Blake, W. H., Smith, H. G., Lizaga, I., & Navas, A. (2019). Testing the sensitivity of a multivariate mixing model using geochemical fingerprints with artificial mixtures. *Geoderma*, *337*, 498–510. https://doi.org/10.1016/j.geoderma.2018.10.005

Haddadchi, A., Olley, J., & Laceby, P. (2014). Accuracy of mixing models in predicting sediment source contributions. *Science of the Total Environment*, *497-498*, 139–152. https://doi.org/10.1016/j.scitotenv.2014.07.105

Han, Z., Wang, X., Song, D., Li, X., Huang, P., & Ma, M. (2019). Response of soil erosion and sediment sorting to the transport mechanism on a steep rocky slope. *Earth Surface Processes and Landforms*, *44*(12), 2467–2478. https://doi.org/10.1002/esp.4675

Knox, N. M., Grunwald, S., McDowell, M. L., Bruland, G. L., Myers, D. B., & Harris, W. G. (2015). Modelling soil carbon fractions with visible near-infrared (VNIR) and mid-infrared (MIR) spectroscopy. *Geoderma*, *239*, 229–239. https://doi.org/10.1016/j.geoderma.2014.10.019

Koiter, A. J., Owens, P. N., Petticrew, E. L., & Lobb, D. A. (2015). The role of gravel channel beds on the particle size and organic matter selectivity of transported fine-grained sediment: Implications for sediment fingerprinting and biogeochemical flux research. *Journal of Soils and Sediments*, *15*(10), 2174–2188. https://doi.org/10.1007/s11368-015-1203-6

Laceby, J. P., Evrard, O., Smith, H. G., Blake, W. H., Olley, J. M., Minella, J. P. G., & Owens, P. N. (2017). The challenges and opportunities of addressing particle size effects in sediment source fingerprinting: A review. *Earth Science Reviews*, *169*, 85–103. https://doi.org/10.1016/j.earscirev.2017.04.009

Laceby, J. P., McMahon, J., Evrard, O., & Olley, J. (2015). A comparison of geological and statistical approaches to element selection for sediment fingerprinting. *Journal of Soils and Sediments*, *15*(10), 2117–2131. https://doi.org/10.1007/s11368-015-1111-9

Lake, N. F., Martínez-Carreras, N., Shaw, P. J., & Collins, A. L. (2022). High frequency un-mixing of soil samples using a submerged spectrophotometer in a laboratory setting—Implications for sediment fingerprinting. *Journal of Soils and Sediments*, *22*(1), 348–364. https://doi.org/10.1007/s11368-021-03107-6

Legout, C., Poulenard, J., Nemery, J., Navratil, O., Grangeon, T., Evrard, O., & Esteves, M. (2013). Quantifying suspended sediment sources during runoff events in headwater catchments using spectrocolorimetry. *Journal of Soils and Sediments*, *13*(8), 1478–1492. https://doi.org/10.1007/s11368-013-0728-9

Madari, B. E., Reeves, J. B., Machado, P. L. O. A., Guimarães, C. M., Torres, E., & McCarty, G. W. (2006). Mid- and near-infrared spectroscopic assessment of soil compositional parameters and structural indices in two Ferralsols. *Geoderma*, *136*(1–2), 245–259. https://doi.org/10.1016/j.geoderma.2006.03.026

Martínez-Carreras, N., Krein, A., Udelhoven, T., Gallart, F., Iffly, J. F., Hoffmann, L., Pfister, L., & Walling, D. E. (2010). A rapid spectral-reflectance-based fingerprinting approach for documenting suspended sediment sources during storm runoff events. *Journal of Soils and Sediments*, *10*(3), 400–413. https://doi.org/10.1007/s11368-009-0162-1

Martínez-Mena, M., Castillo, V., & Albaladejo, J. (2002). Relations between interrill erosion processes and sediment particle size distribution in a semiarid Mediterranean area of SE of Spain. *Geomorphology*, *45*(3), 261–275. https://doi.org/10.1016/S0169-555X(01)00158-1

Ni, L. S., Fang, N. F., Shi, Z. H., & Tan, W. F. (2019). Mid-infrared spectroscopy tracing of channel erosion in highly erosive catchments on the Chinese loess plateau. *Science of the Total Environment*, *687*, 309–318. https://doi.org/10.1016/j.scitotenv.2019.06.116

Ni, L. S., Fang, N. F., Shi, Z. H., Chen, F. X., & Wang, L. (2017). Validating a basic assumption of using Cesium-137 method to assess soil loss in a small agricultural catchment. *Land Degradation and Development*, *28*(5), 1772–1778. https://doi.org/10.1002/ldr.2708

Poesen, J. (2018). Soil erosion in the Anthropocene: Research needs. *Earth Surface Process and Landform*, *43*(1), 64–84. https://doi.org/10.1002/esp.4250

Poulenard, J., Legout, C., Némery, J., Bramorski, J., Navratil, O., Douchin, A., Fanget, B., Perrette, Y., Evrard, O., & Esteves, M. (2012). Tracing sediment sources during floods using diffuse reflectance infrared Fourier transform spectrometry (DRIFTS): A case study in a highly erosive mountainous catchment (southern French Alps). *Journal of Hydrology*, *414-415*, 452–462. https://doi.org/10.1016/j.jhydrol.2011.11.022

Poulenard, J., Perrette, Y., Fanget, B., Quetin, P., Trevisan, D., & Dorioz, J. M. (2009). Infrared spectroscopy tracing of sediment sources in a small rural watershed (French Alps). *Science of the Total Environment*, *407*(8), 2808–2819. https://doi.org/10.1016/j.scitotenv.2008.12.049

Pulley, S., & Collins, A. L. (2022). A rapid and inexpensive colour-based sediment tracing method incorporating hydrogen peroxide sample treatment as an alternative to quantitative source fingerprinting for catchment management. *Journal of Environmental Management*, *311*, 114780. https://doi.org/10.1016/j.jenvman.2022.114780

Pulley, S., & Rowntree, K. (2016). The use of an ordinary colour scanner to fingerprint sediment sources in the south African Karoo. *Journal of Environmental Management*, *165*, 253–262. https://doi.org/10.1016/j.jenvman.2015.09.037

Rossel, R. V., & Behrens, T. (2010). Using data mining to model and interpret soil diffuse reflectance spectra. *Geoderma*, *158*(1–2), 46–54. https://doi.org/10.1016/j.geoderma.2009.12.025

Sellier, V., Navratil, O., Laceby, J. P., Legout, C., Foucher, A., Allenbach, M., Lefèvre, I., & Evrard, O. (2021). Combining colour parameters and geochemical tracers to improve sediment source discrimination in a mining catchment (New Caledonia, South Pacific Islands). *The Soil*, *7*(2), 743–766. https://doi.org/10.5194/soil-7-743-2021

Sherriff, S. C., Franks, S. W., Rowan, J. S., Fenton, O., & Ó HUallacháin, D. (2015). Uncertainty-based assessment of tracer selection, tracer non-conservativeness and multiple solutions in sediment fingerprinting using synthetic and field data. *Journal of Soils and Sediments*, *15*(10), 2101–2116. https://doi.org/10.1007/s11368-015-1123-5

Shi, W. Y., Yue, R., & Fang, N. F. (2019). A review of researches on sediment sources discrimination with composite fingerprinting techniques in loess plateau. *Bulletin of Soil and Water Conservation*, *39*(3), 276–285. https://doi.org/10.13961/j.cnki.stbctb.2019.03.045

Soil Survey Staff. (2010). *Keys to taxonomy* (Eleventh ed.). United States Department of Agriculture.

Soriano-Disla, J. M., Janik, L. J., Viscarra Rossel, R. A., Macdonald, L. M., & McLaughlin, M. J. (2014). The performance of visible, near-, and mid-infrared reflectance spectroscopy for prediction of soil physical, chemical, and biological properties. *Applied Spectroscopy Reviews*, *49*(2), 139–186. https://doi.org/10.1080/05704928.2013.811081

Stock, B. C., Jackson, A. L., Ward, E. J., Parnell, A. C., Phillips, D. L., & Semmens, B. X. (2018). Analyzing mixing systems using a new generation of Bayesian tracer mixing models. *PeerJ*, *6*, e5096. https://doi.org/10.7717/peerj.5096

Syvitski, J., Ángel, J. R., Saito, Y., Overeem, I., Vörösmarty, C. J., Wang, H., & Olago, D. (2022). Earth's sediment cycle during the Anthropocene Nature Reviews. *Earth and Environment*, *3*(3), 179–196. https://doi.org/10.1038/s43017-021-00253-w

Tiecher, T., Caner, L., Minella, J. P. G., & Santos, D. R. D. (2015). Combining visible-based-color parameters and geochemical tracers to improve sediment source discrimination and apportionment. *Science of the Total Environment*, *527-528*, 135–149. https://doi.org/10.1016/j.scitotenv.2015.04.103

Tiecher, T., Caner, L., Minella, J. P. G., Bender, M. A., & Dos Santos, D. R. (2016). Tracing sediment sources in a subtropical rural catchment of southern Brazil by using geochemical tracers and near-infrared spectroscopy. *Soil and Tillage Research*, *155*, 478–491. https://doi.org/10.1016/j.still.2015.03.001

Tiecher, T., Caner, L., Minella, J. P. G., Evrard, O., Mondamert, L., Labanowski, J., & Rheinheimer, D. D. S. (2017). Tracing sediment sources using mid-infrared spectroscopy in Arvorezinha catchment, Southern Brazil. *Land Degradation and Development*, *28*(5), 1603–1614. https://doi.org/10.1002/ldr.2690

Tiecher, T., Moura-Bueno, J. M., Caner, L., Minella, J. P. G., Evrard, O., Ramon, R., Naibo, G., Barros, C. A. P., Silva, Y. J. A. B., Amorim, F. F., & Rheinheimer, D. S. (2021). Improving the quantification of sediment source contributions using different mathematical models and spectral preprocessing techniques for individual or combined spectra of ultraviolet–visible, near- and middle-infrared spectroscopy. *Geoderma*, *384*, 114815. https://doi.org/10.1016/j.geoderma.2020.114815

Vale, S. S., Fuller, I. C., Procter, J. N., Basher, L. R., & Smith, I. E. (2016). Characterization and quantification of suspended sediment sources to the Manawatu River, New Zealand. *Science of the Total Environment*, *543*, 171–186. https://doi.org/10.1016/j.scitotenv.2015.11.003

Vale, S., Swales, A., Smith, H. G., Olsen, G., & Woodward, B. (2022). Impacts of tracer type, tracer selection, and source dominance on source apportionment with sediment fingerprinting. *Sci Total Environ*, *831*, 154832. https://doi.org/10.1016/j.scitotenv.2022.154832

Vercruysse, K., & Grabowski, R. C. (2018). Using source-specific models to test the impact of sediment source classification on sediment fingerprinting. *Hydrological Processes*, *32*(22), 3402–3415. https://doi.org/10.1002/hyp.13269

Verheyen, D., Diels, J., Kissi, E., & Poesen, J. (2014). The use of visible and near-infrared reflectance measurements for identifying the source of suspended sediment in rivers and comparison with geochemical fingerprinting. *Journal of Soils and Sediments*, *14*(11), 1869–1885. https://doi.org/10.1007/s11368-014-0938-9

Viscarra Rossel, R. A., Minasny, B., Roudier, P., & McBratney, A. B. (2006). Colour space models for soil science. *Geoderma*, *133*(3–4), 320–337. https://doi.org/10.1016/j.geoderma.2005.07.017

Walling, D. E. (2005). Tracing suspended sediment sources in catchments and river systems. *Science of the Total Environment*, *344*(1–3), 159–184. https://doi.org/10.1016/j.scitotenv.2005.02.011

Wang, L., Huang, X., Fang, N. F., Niu, Y. H., Wang, T. W., & Shi, Z. H. (2019). Selective transport of soil organic and inorganic carbon in eroded sediment in response to raindrop sizes and inflow rates in rainstorms. *Journal of Hydrology*, *575*, 42–53. https://doi.org/10.1016/j.jhydrol.2019.05.033

Xu, Z., Belmont, P., Brahney, J., & Gellis, A. C. (2022). Sediment source fingerprinting as an aid to large-scale landscape conservation and restoration: A review for the Mississippi River basin. *Journal of Environmental Management*, *324*, 116260. https://doi.org/10.1016/j.jenvman.2022.116260

Yang, D., Fang, N., Shi, Z., Lin, J., & Zong, R. (2022). Modeling sediment transport and flow velocity of thawed soil with straw returning. *Journal of Hydrology*, *610*, 127805. https://doi.org/10.1016/j.jhydrol.2022.127805

Zhang, J. Q., Wang, X. T., Yang, M. Y., Liu, Y., Zhang, F. B., & Ying, M. F. (2021). Effect of particle sorting and organic matter on sediment source study using composite fingerprints. *Scientia Geographica Sinica*, *41*(3), 504–512. https://doi.org/10.13249/j.cnki.sgs.2021.03.015

How to cite this article: Chen, D., Dai, W., Li, M., Wang, B., Zeng, Y., Ni, L., Fang, N., & Shi, Z. (2023). Accuracy verification of optical fingerprinting methods in sediment tracing study. *Hydrological Processes*, *37*(4), e14870. https://doi.org/10.1002/hyp.14870